Available online at www.sciencedirect.com
ScienceDirect
Composites Science and Technology 68 (2008) 1704–1709
COMPOSITES SCIENCE AND TECHNOLOGY
www.elsevier.com/locate/compscitech

Electrospun $MnFe_2O_4$ nanofibers: Preparation and morphology

Young-Wan Ju [a], Jae-Hyun Park [a,b], Hong-Ryun Jung [a], Sung-June Cho [a,b], Wan-Jin Lee [a,b,*]

[a] Faculty of Applied Chemical Engineering, Chonnam National University, 300 Yongbong-dong, Buk-gu, Gwangju 500-757, Republic of Korea
[b] Center for Functional Nano Fine chemicals(BK21), Chonnam National University, 300 Yongbong-dong, Buk-gu, Gwangju 500-757, Republic of Korea

Received 29 June 2007; received in revised form 18 December 2007; accepted 6 February 2008
Available online 10 March 2008

Abstract

The composite fibers were prepared by an electrospinning the solutions mixed manganese ferrite sol with polyvinyl acetate (PVAc). The manganese ferrite sol was obtained from manganese(II) nitrate and iron(III) nitrate nonahydrate molecular precursor based on a sol–gel procedure. Manganese ferrite ($MnFe_2O_4$) nanofibers were prepared by calcining the above composite fibers in air at 400, 600 and 800 °C, respectively. The obtained nanofibers were characterized by SEM, FT-IR, XRD, and extended X-ray absorption fine structure (EXAFS). After being calcined at 800 °C, the fibers became continuous crystallites as a result of the complete decomposition of PVAc. The morphology of manganese ferrite was found to be cubic spinel structure containing eight oxygens and 12 metal atoms in the unit cell, referred from the results of EXAFS. Also, the magnetic properties of the calcined samples were characterized by using a vibrating sample magnetometer (VSM).

Keywords: A. Nano composites; E. Electrospinning; E. Annealing; E. Sol–gel methods

1. Introduction

Manganese ferrite ($MnFe_2O_4$) has received a great attention in the area of magnetic storage device, microwave, and electronic device because it has high magnetic permeability and high electrical resistance. Many research groups have investigated to enhance the magnetic property of magnetic materials such as manganese ferrite. The nanoparticles of manganese ferrite have been prepared employing several methods such as ball-milling [1–3], co-precipitation [4–7], reverse micelle synthesis [8], pulsed laser deposition [9], solid-phase reactions [10], thermal decomposition [11], and sol–gel method [12,13]. Also, the nanorods and nanowires of manganese ferrite have synthesized using a low-temperature hydrothermal process in order to enhance the magnetic property. The magnetic property depends on the morphology. The nanorods have a good magnetic property because it has easy grown along the magnetization axis [14,15].

We introduce the preparation of manganese ferrite by electrospinning process as a method to increase the magnetic property. The evidence of preparation of manganese ferrite by electrospinning technique is hard to find elsewhere. Electrospinning is a unique method of making nanofibers [16,17], metal oxide nanofibers [18–20], carbon nanofibers [21,22] and metal embedded carbon nanofibers [23] within electromagnetic field to apply the proper voltage so as to overcome the surface tension of solution. The morphology of the fibers is largely affected by viscosity of solution, applied electric field strength, the distance between a syringe and collector. The fibers prepared by electrospinning have good orientation, large specific surface area, large aspect ratio, and dimensional stability.

An aim of this study is to prepare the cubic spinel manganese ferrite ($MnFe_2O_4$) nanofibers through electrospinning process of sol–gel solutions. The nanofibers of

* Corresponding author. Address: Faculty of Applied Chemical Engineering, Chonnam National University, 300 Yongbong-dong, Buk-gu, Gwangju 500-757, Republic of Korea. Tel.: +82 62 530 1895; fax: +82 62 530 1889.
E-mail address: wjlee@chonnam.ac.kr (W.-J. Lee).

0266-3538/$ - see front matter © 2008 Elsevier Ltd. All rights reserved.
doi:10.1016/j.compscitech.2008.02.015

manganese ferrite were characterized by TGA, FE-SEM, XRD, FT-IR, vibrating sample magnetometer (VSM) and extended X-ray absorption fine structure (EXAFS).

2. Experimental

2.1. Materials

Manganese(II) nitrate (45–50 wt% solution in dilute nitric acid, Aldrich Chemical Co.) and iron(III) nitrate nonahydrate (99%, Aldrich Chemical Co.) were used as metal precursors. Citric acid anhydrous ($C_3H_4(OH)(COOH)_3$, 99.5%, Yakuri Pure Chemical Co.) was employed as a chelating agent. Poly(vinyl acetate) (PVAc, Mw = 500,000) was purchased from Aldrich Chemical Co., *N*,*N*-dimethylformamide (DMF, 99.5%, Duksan Chemical Co.) and tetrahydrofuran (THF, 99.5%, Duksan Chemical Co.) were used as solvents.

2.2. Preparation of $MnFe_2O_4$/PVAc solution

PVAc (15 wt%) solution was prepared using DMF/THF (4:6 by weight ratio) as co-solvent. The manganese ferrite sol was obtained from the dissolution iron(III) nitrate nonahydrate (2.02 g), manganese(II) nitrate (0.6 ml) and acetic acid (3 g) were dissolved in distilled water (15 ml). The following evaporation of water resulted in the formation of the gel. The electrospinning solution was obtained by mixing PVAc solution with manganese ferrite gel (1.5:1.0 by weight ratio) under vigorous stirring for 12 h.

2.3. Preparation of $MnFe_2O_4$/PVAc nanofiber composites

Fig. 1 shows the experimental apparatus used for electrospinning with power supply (NT-PS-35K, NTSEE, Korea) of a variable high voltage. A composite solution was placed in a 30 ml syringe with a positively charged capillary tip with a diameter of 0.5 mm. The anode of the high voltage power supply was clamped to a syringe needle tip and the cathode was connected to a metal collector. The electrospun nanofiber composite web was collected by attaching it to aluminum foil wrapped on a metal drum rotating at approximately 300 rpm. The applied voltage was 20 kV, the distance between the syringe needle tip and collector was 18 cm, and the flow rate of the spinning solution was 1 ml/h. The electrospun fibers were dried by heating them at 80 °C for 6 h in an air atmosphere. The dried fibers were calcined at 400, 600 and 800 °C, respectively for 4 h in an air gas to get manganese ferrite fibers with a heating rate of 1 °C /min.

2.4. Characterization of $MnFe_2O_4$/PVAc nanofiber composite

The micro-texture of the nano-structured materials was examined by scanning electron microscopy (SEM, Hitachi, S-4700, Japan). The thermal properties of the electrospun manganese ferrite fibers were characterized by thermogravimetric analysis (TGA, Stanton Redcroft, STA1640, England) at a heating rate of 10 °C/min in nitrogen atmosphere. The X-ray diffraction (XRD) patterns were obtained using a D/MAX Uitima III (Rigaku, Japan). FT-IR spectra of the samples (as pellets in KBr) have been recorded by the Nicolet 520P (Nicolet, USA). Extended X-ray absorption fine structure (EXAFS) of the sample was obtained under ambient conditions using R-XAS instrument (Rigaku, Japan) operating at 20 kV and 15 mA with a W filament, and also at Beamline 3C1 in the Pohang Accelerator Laboratory, Korea. The data was analyzed by the standard method using the *ab initio* Feff program [24]. Magnetic measurements were carried out at room temperature using a vibrating sample magnetometer (VSM, Lake Shore 7300, KBSI-PA306).

3. Results and discussion

Fig. 2 shows TGA thermograms of pure PVAc fibers and manganese ferrite/PVAc composite fibers. As shown

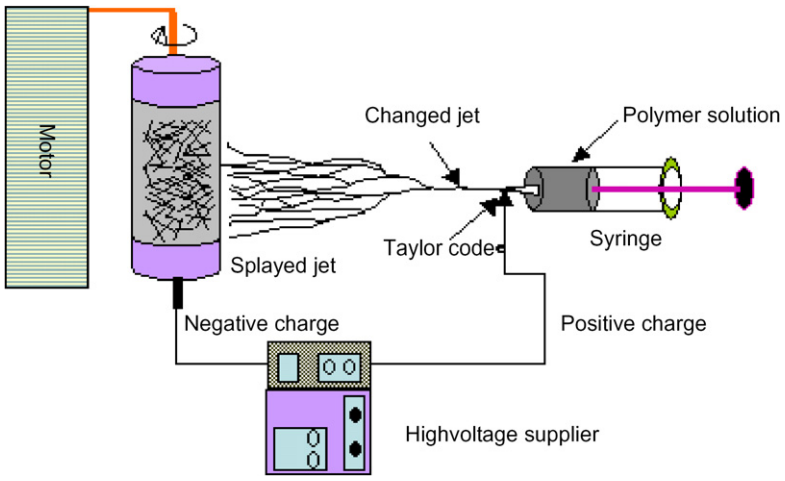

Fig. 1. Schematic drawing of the electrospinning process.

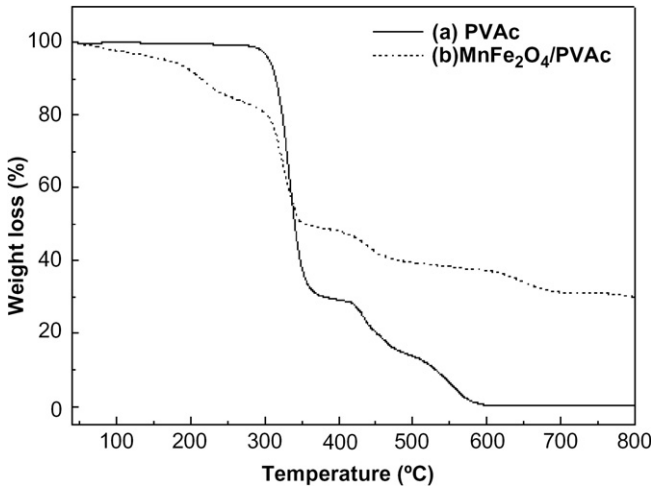

Fig. 2. TGA thermograms of (a) pure PVAc fibers, (b) and manganese ferrite/PVAc composite fibers.

in Fig. 2a, pure PVAc decomposed up to about 70% at 400 °C, and completely at above 600 °C. In Fig. 2b, the composite fibers degrade through three steps. The first step of weight loss corresponded to the evaporation of water and solvent in the range of 25–200 °C. The second weight loss was due to the degradation of PVAc side chain between 200 and 300 °C. The last step occurred above 300 °C because of further decomposition of PVAc main chain.

Fig. 3 shows SEM images of electrospun $MnFe_2O_4$ fibers. The diameter of fibers was slightly decreased with increasing the calcined temperature. It can be seen in Fig. 3a that the as-prepared composite fibers are partially aligned along the winding direction of the drum winder. The surface of fibers is smooth and uniform and the resulting diameter is 200 ± 20 nm, on the average. As shown in Fig. 3b and c, the fibers calcined at 400 and 600 °C are shrunk with wrinkles due to the decomposition of PVAc. After being calcined at 800 °C as shown in Fig. 3d, the fibers become continuous crystallites of an average diameter of 180 ± 20 nm due to the complete decomposition of PVAc.

Fig. 4 presents the XRD patterns of fibers with various calcined temperatures. A XRD pattern of as-prepared composite fiber as shown in Fig. 4a corresponds to that of the typical amorphous structure. After being calcined at 400 °C as shown in Fig. 4b, the $MnFe_2O_4$ spinel (JCPDS card no. 10-0319) phase starts to appear at $2\theta = 30°$, 35°, 42°, 52°, 56° and 61°. However, the crystallization is low.

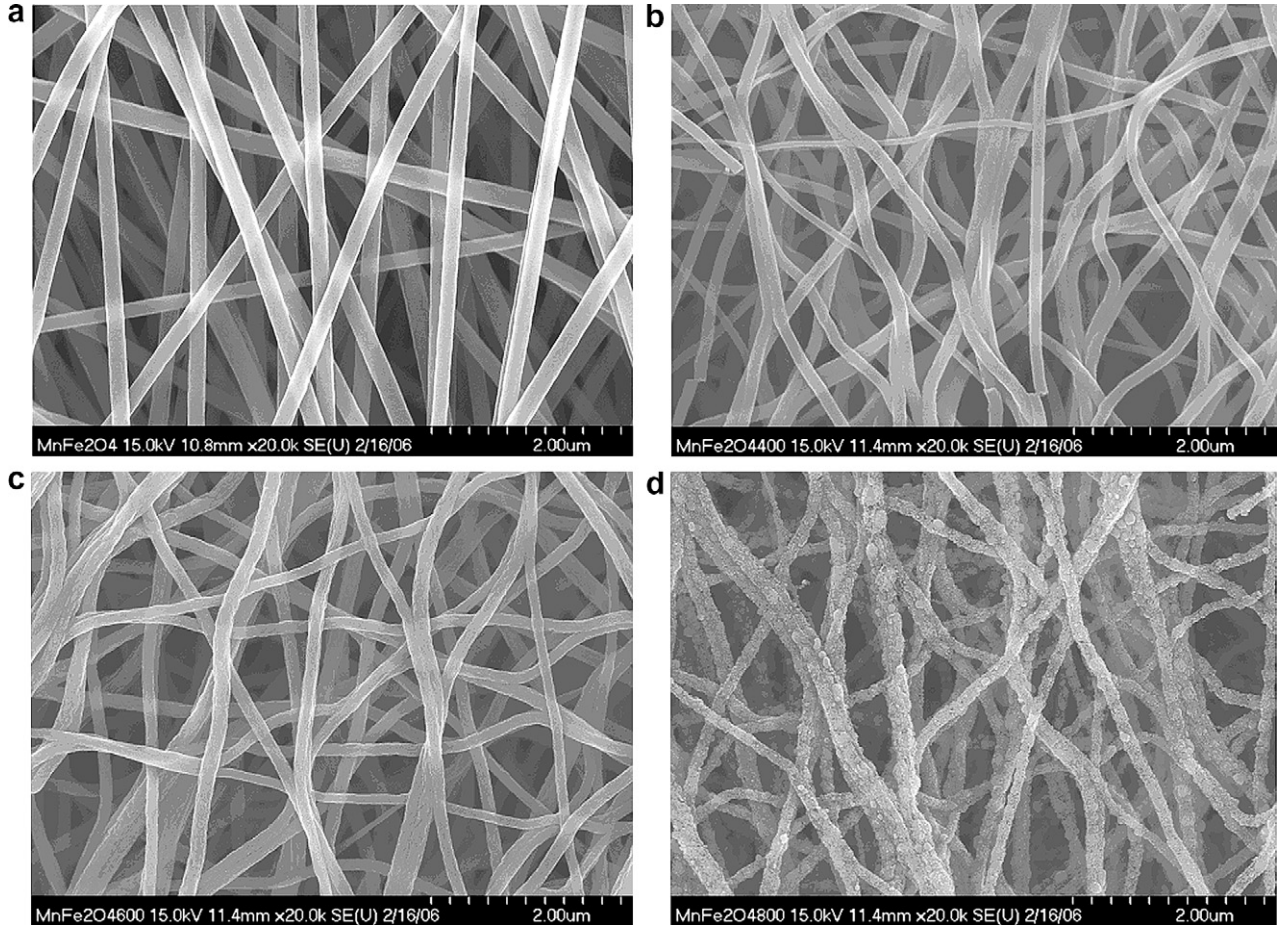

Fig. 3. SEM images of manganese ferrite/PVAc composite fibers; (a) as-prepared composite fibers, (b) fibers calcined at 400 °C, (c) fibers calcined at 600 °C, and (d) fibers calcined at 800 °C.

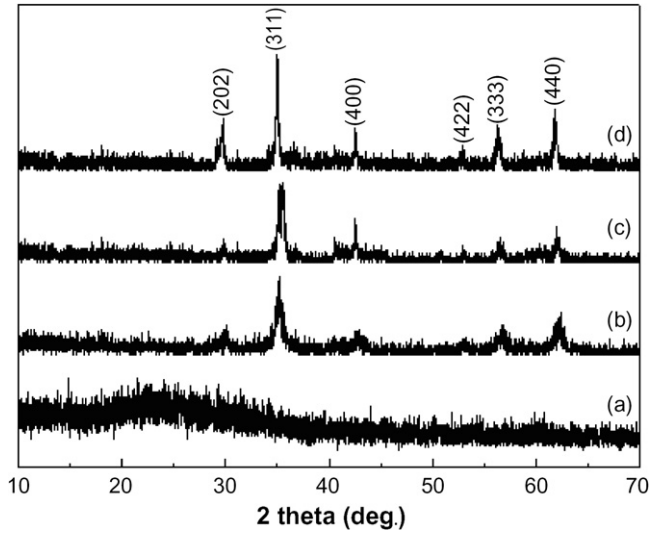

Fig. 4. XRD patterns of manganese ferrite/PVAc composite fibers; (a) as-prepared composite fibers, (b) fibers calcined at 400 °C, (c) fibers calcined at 600 °C, and (d) fibers calcined at 800 °C.

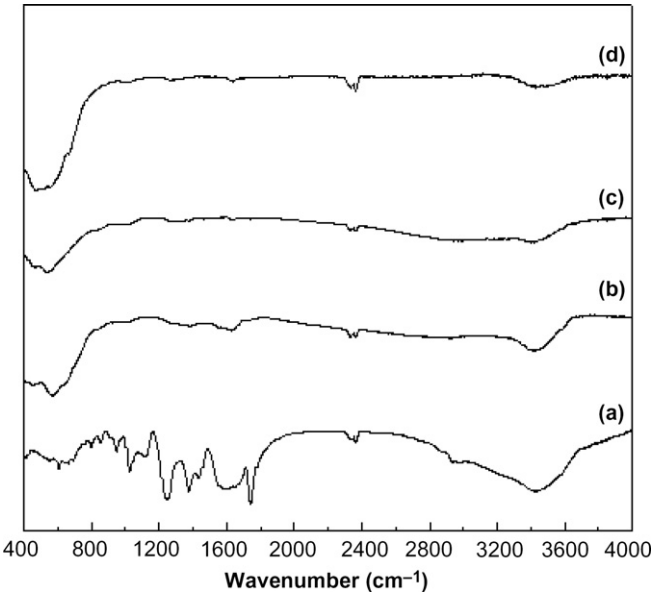

Fig. 5. FT-IR spectra of manganese ferrite/PVAc composite fibers; (a) as-prepared composite fibers, (b) fibers calcined at 400 °C, (c) fibers calcined at 600 °C, and (d) fibers calcined at 800 °C.

Table 1
The lattice parameter, average size of crystallites calculated from XRD results, and magnetic properties with the calcined temperature

Calcination temperature (°C)	Lattice parameter (Å)	Average size of crystallites (Å)	Magnetization at 10 kOe (emu/g)	Mr[a] (emu/g)	He[b] (Oe)
600	8.3696	2.8177	46.8	13.4	607.7
800	8.3912	3.1352	61.14	17.5	642.6

[a] Mr: ketenuvity or samples.
[b] Hc: coercivity of samples.

As the calcined temperature is increased, the crystallization is to be developed. The $MnFe_2O_4$ nanofibers calcinated at 800 °C as shown in Fig. 4d become fully crystalline composites. The cubic spinel lattice parameter (a) and the average size of the crystallites are summarized in Table 1. The lattice parameter was calculated by using the full width at half-maximum (FWHM) of the peak (3 1 1) from the Eq. (1), and θ was 17.718° at (3 1 1) plane. The hkl index was based on the PDF card no. 10-0319.

$$\sin^2\theta = \left(\frac{\lambda^2}{4a^2}\right)(h^2 + k^2 + t^2) \quad (1)$$

The average size of the crystallites ($B_{\text{crystallite}}$), also, was calculated by using FWHM of the peak (3 1 1) from the Scherrer's equation, as described by Eq. (2).

$$B_{\text{crystallite}} = \frac{k\lambda}{L\cos\theta} \quad (2)$$

The lattice parameter and average size of the crystallites increased as the calcined temperature increased. The $MnFe_2O_4$ spinel structure was confirmed by EXAFS.

Fig. 5 shows FT-IR spectra of fibers as a function of the calcined temperature. The strong absorption peaks of as-prepared composite fibers, as shown in Fig. 5a, ranged from 600 to 3600 cm^{-1} owing to the stretching and bending vibrations of PVAc. Specifically, the C=O stretching peak of unconjugated ester appears at about 1736 cm^{-1}, the methyl group peak of ester displays at around 1375 cm^{-1}, and the C–O stretching peak of ester represents at about 1239 cm^{-1} [25]. As the calcined temperature increases, most of organic peaks disappear due to the decomposition of PVAc. It is very interesting to note two peaks, that is, the disappearance of O–H peak and the formation of new peak. As the calcined temperature increases, the O–H peak of around 3428 cm^{-1} is gradually disappeared, while the new peak formed at the range of 500–700 cm^{-1} by the progress of crystallization becomes stronger and narrower [26]. In detail, the new band between 500 and 700 cm^{-1} becomes narrow further due to the crystallization with the increase of the temperature up to 800 °C.

k^3-weighted EXAFS spectrum and its corresponding Fourier transform of the manganese ferrite (MnFe2O4) calcined at 800 °C are shown in Fig. 6a and b, respectively. Table 2 shows the structural parameter of manganese ferrite (MnFe2O4) obtained through the non-linear least square curve fitting using UWXAFS2 and Feff8 [27,28]. The result of Table 2 suggests the presence of cubic spinel structure as shown in Fig. 7, based on the results of atomic distance and coordination number. The cubic spinel structure in MnFe2O4 has coordination numbers of 4 O, 3 Fe and 3 Mn atoms around the Fe atom, and also 4 O, 3 Mn and 3 Fe around the Mn atom. In other words, the morphology of manganese ferrite is formed as the cubic spinel structure containing eight oxygens and 12 metal atoms in the unit cell. The total coordination number around the specific absorber was consistent with the theoretical value within error limit.

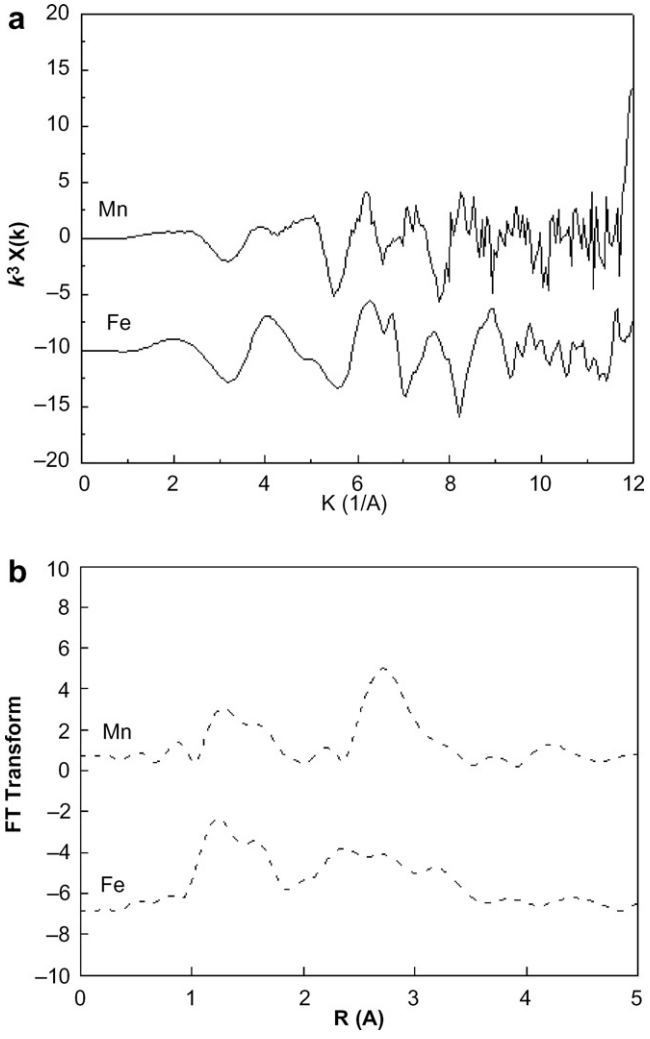

Fig. 6. (a) k^3-weighted EXAFS spectrum and (b) its corresponding Fourier transform of the manganese ferrite ($MnFe_2O_4$) calcined at 800 °C. The dotted line indicated the best fitted EXAFS function.

Fig. 8 represents magnetic hysteresis loops of the samples calcined at 600 °C (a) and 800 °C (b), measured at room temperature. Both samples illustrated the typical hys-

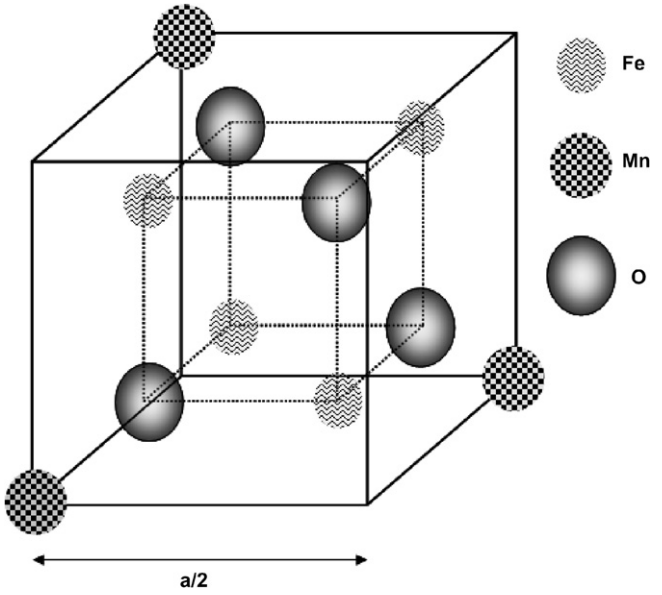

Fig. 7. Morphology of $MnFe_2O_4$ by EXAFS analysis.

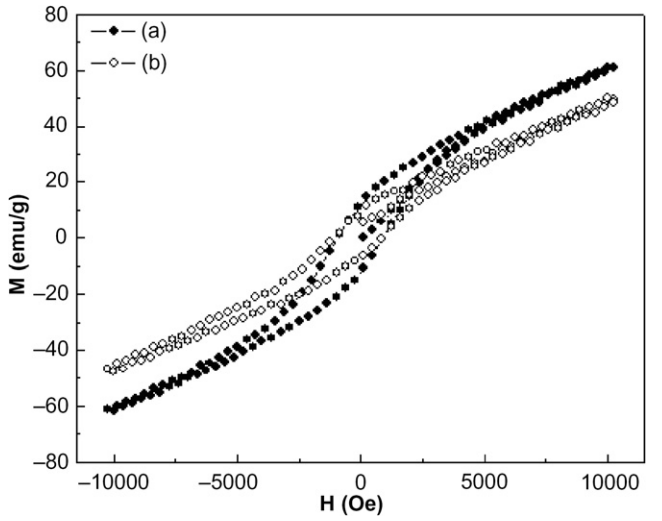

Fig. 8. M–H (magnetization–hysteresis) loops of the samples calcined at 600 °C (a) and 800 °C (b), measured at room temperature.

Table 2
Structural parameters obtained from the curve fitting of EXAFS spectrum of the manganese ferrite/PVAc composite fibers calcined at 800 °C, obtained at the Mn and Fe *K*-edge and room temperature

Sample	Shell	N[a]	R (Å)[b]	σ^2 (Å)[c]	£o (eV)
$MnFe_2O_4$–Fe	Fe–O	1.2(0.1488)	1.86(0.0319)	0.0015(0.0033)	−1.61(0.8210)
	Fe–O	4.4(0.3421)	2.01(0.0146)	0.0106(0.0022)	
	Fe–Fe	0.7(0.3669)	2.56(0.0159)	0.0013(0.0026)	
	Fe–Mn	5.0(1.8857)	3.02(0.0144)	0.0144(0.0047)	
	Fe–Fe	1.5(0.2903)	3.34(0.0144)	0.0024(0.0020)	
$MnFe_2O_4$– Mn	Mn–O	0.5(0.1841)	1.75(0.1503)	0.0011(0.0139)	−4.57(0.5430)
	Mn–O	1.9(0.12165)	1.93(0.0142)	0.0016(0.0018)	
	Mn–Mn	3.2(0.3637)	3.10(0.0073)	0.0047(0.0012)	
	Mn–Fe	2.0(0.8413)	3.56(0.0189)	0.0057(0.0043)	

[a] Coordination number.
[b] Atomic distance.
[c] The Debye–Wallet factor.

teresis loops of magnetic behaviors. In this study, the characterization that an ordered magnetic system of manganese ferrite is the cubic spinel structure is confirmed by EXAFS, as explained earlier. Magnetization data are listed in Table 1. The saturation magnetization for the sample calcined at 800 °C represented around 61 emu g^{-1} at 10 kOe, representing slightly small value compared to that of bulk manganese ferrite, known as 80 emu g^{-1} [5]. The reason for this is originated from the nature of ultrafine particles such as surface disorder and defects. The remanence and coercivity of sample calcined at 800 °C were 17.8 emu g^{-1}, and 642.6 Oe, while those of sample calcined at 600 °C were 13.4 emu g^{-1} and 607.7 Oe. It is derived from the rise of the particle size.

4. Conclusions

Manganese ferrite ($MnFe_2O_4$)/polyvinyl acetate (PVAc) composite fibers were prepared by an electrospinning technique using sol–gel precursors, and $MnFe_2O_4$ fibers were synthesized by calcining with various temperatures. The diameters of $MnFe_2O_4$ nanofibers calcinded at 800 °C ranged from 160 to 200 nm. Also, the structure of $MnFe_2O_4$ nanofibers was changed from amorphous phase to crystalline phase with increasing temperature. The manganese ferrite was formed as the cubic spinel structure, as confirmed by XRD and EXAFS. Magnetization, remanence and coercivity increased with increasing the calcined temperature. It is expected that $MnFe_2O_4$ fibers fabricated by electrospinning can be used as magnetic materials such as magnetic recording device, magneto-optical recording, and electronic devices.

Acknowledgements

This work was supported by the Korea Foundation for International Cooperation of Science and Technology (KICOS) through a Grant provided by the Korean Ministry of Science and Technology (MOST) in K20602000009-07E0200-00910.

References

[1] Mahmoud MH, Hamdeh HH, Ho JC, O'Shea MJ, Walker JC. Mössbauer studies of manganese ferrite fine particles processed by ball-milling. J Magn Magn Mater 2000;220(2–3):139–46.
[2] Muroi M, Street R, McCormick PG, Amighian J. Magnetic properties of ultrafine $MnFe_2O_4$ powders prepared by mechanochemical processing. Phys Rev B 2001;63:184414.
[3] Ding J, McCormick PG, Street R. Formation of spinel Mn-ferrite during mechanical alloying. J Magn Magn Mater 1997;171(3):309–14.
[4] Kulkarni GU, Kannan KR, Arunarkavalli T, Rao CNR. Particle-size effects on the value of T_c of $MnFe_2O_4$: evidence for finite-size scaling. Phys Rev B 1994;49:724–7.
[5] Tang ZX, Sorensen CM, Klabunde KJ, Hadjipanayis GC. Size-dependent Curie temperature in nanoscale $MnFe_2O_4$ particles. Phys Rev Lett 1991;67:3602–5.
[6] Tang ZX, Chen JP, Sorensen CM, Klabunde KJ, Hadjipanayis GC. Phys Rev Lett 1992;68:3114.
[7] Chen JP, Sorensen CM, Klabunde KJ, Hadjipanayis GC, Devlin E, Kostikas A. Size-dependent magnetic properties of $MnFe_2O_4$ fine particles synthesized by coprecipitation. Phys Rev B 1996;54:9288–96.
[8] Liu C, Zhang ZJ. Size-dependent superparamagnetic properties of Mn spinel ferrite nanoparticles synthesized from reverse micelles. Chem Mater 2001;13:2092–6.
[9] Mahmouda MH, Williams CM, Cai J, Siu I, Walker JC. Investigation of Mn-ferrite films produced by pulsed laser deposition. J Magn Magn Mater 2003;261:314–8.
[10] Deraz NM, El-Shobaky GA. Solid-solid interaction between ferric oxide and manganese carbonate as influenced by lithium oxide doping. Thermochim Acta 2001;375:137–45.
[11] Balaji G, Gajbhiye NS, Wilde G, Weissmuller J. Magnetic properties of $MnFe_2O_4$ nanoparticles. J Magn Magn Mater 2002;242-245:617–20.
[12] Schleich DM, Zhang Y. Preparation of some metal ferrite MFe_2O_4 thin films through a nonaqueous sol method. Mater Res Bull 1995;30:447–52.
[13] Gajbhiye NS, Balaji G. Synthesis, reactivity, and cations inversion studies of nanocrystalline $MnFe_2O_4$ particles. Thermochim Acta 2002;385(1-2):143–51.
[14] Wang J, Chen Q, Hou B, Peng Z. Synthesis and magnetic properties of single-crystals of $MnFe_2O_4$ nanorods. Eur J Inorg Chem 2004;6:1165–8.
[15] Li Y, Yin XF, Chen FR, Yang HH, Zhuang ZX, Wang XR. Synthesis of magnetic molecularly imprinted polymer nanowires using a nanoporous alumina template. Macromolecules 2006;39:4497–9.
[16] Moroni L, Licht R, Boer J, Wijn JR, van Blitterswijk CA. Fiber diameter and texture of electrospun PEOT/PBT scaffolds influence human mesenchymal stem cell proliferation and morphology, and the release of incorporated compounds. Biomaterials 2006;27:4911–22.
[17] Ahn YC, Park SK, Kim GT, Hwang YJ, Lee CG, Shin HS, et al. Development of high efficiency nanofilters made of nanofibers. Curr Appl Phys 2006;6:1030–5.
[18] Li D, Herricks T, Xia Y. Magnetic nanofibers of nickel ferrite prepared by electrospinning. Appl Phys Lett 2003;83:4586–8.
[19] Zhu Y, Zhang JC, Zhai J, Zheng YM, Feng L, Jiang L. Multifunctional carbon nanofibers with conductive, magnetic and superhydrophobic properties. Chem Phys Chem 2006;7:336–41.
[20] Yuh J, Nino JC, Sigmund WM. Synthesis of barium titanate ($BaTiO_3$) nanofibers via electrospinning. Mater Lett 2005;59:3645–7.
[21] Kim C, Park SH, Lee WJ, Yang KS. Characteristics of supercapacitor electrodes of PBI-based carbon nanofiber web prepared by electrospinning. Electrochim Acta 2004;50:877–81.
[22] Kim C, Choi YO, Lee WJ, Yang KS. Supercapacitor performances of activated carbon fiber webs prepared by electrospinning of PMDA-ODA poly(amic acid) solutions. Electrochim Acta 2004;50:883–7.
[23] Ju YW, Choi GR, Jung HR, Kim C, Yang KS, Lee WJ. A hydrous ruthenium oxide-carbon nanofibers composite electrodes prepared by electrospinning. J Electrochem Soc 2007;154:A192–7.
[24] Rehr JJ, Albers RC, Zabinsky SI. High-order multiple-scattering calculations of X-ray-absorption fine structure. Phys Rev Lett 1992;69:3397–400.
[25] Sharma L, Kimura T. FT-IR investigation into the miscible interaction in new materials for optical devices. Polym Adv Technol 2003;14:392–9.
[26] Rajić N, Čeh M, Gabrovšek R, Kaučič V. Formation of nanocrystalline transition-metal ferrites inside of silica matrix. J Am Ceram Soc 2002;85:1719–24.
[27] Stern EA, Newville M, Ravel B, Yacoby Y, Haskel D. The UWXAFS analysis package: philosophy and details. Physica B 1995;208:117–20.
[28] Newville M, Livins P, Yacoby Y, Rehr JJ, Stern EA. Near-edge X-ray absorption fine structure of Pb: a comparison of theory and experiment. Phys Rev B 1993;47:14126–31.